Tuning Metal–Organic Frameworks with Open-Metal Sites and Its Origin for Enhancing CO2 Affinity by Metal Substitution

ARTICLE *in* JOURNAL OF PHYSICAL CHEMISTRY LETTERS · MARCH 2012

Impact Factor: 7.46 · DOI: 10.1021/jz300047n

4 AUTHORS, INCLUDING:

Joonho Park
Korea Advanced Institute of Science and Tech…
20 PUBLICATIONS **382** CITATIONS
SEE PROFILE

Heejin Kim
Korea Basic Science Institute KBSI
14 PUBLICATIONS **422** CITATIONS
SEE PROFILE

Sang Soo Han
Korea Research Institute of Standards and Sci…
58 PUBLICATIONS **1,900** CITATIONS
SEE PROFILE

THE JOURNAL OF PHYSICAL CHEMISTRY Letters

Letter

pubs.acs.org/JPCL

Tuning Metal–Organic Frameworks with Open-Metal Sites and Its Origin for Enhancing CO_2 Affinity by Metal Substitution

Joonho Park,[†] Heejin Kim,[†] Sang Soo Han,[‡] and Yousung Jung*[,†]

[†]Graduate School of EEWS (WCU), Korea Advanced Institute of Science and Technology (KAIST), Daejeon 305-701, Korea

[‡]Center for Nanocharacterization, Korea Research Institute of Standards and Science, Daejeon 305-340, Korea

Supporting Information

ABSTRACT: Reducing anthropogenic carbon emission is a problem that requires immediate attention. Metal–organic frameworks (MOFs) have emerged as a promising new materials platform for carbon capture, of which Mg-MOF-74 offers chemospecific affinity toward CO_2 because of the open Mg sites. Here we tune the binding affinity of CO_2 for M-MOF-74 by metal substitution (M = Mg, Ca, and the first transition metal elements) and show that Ti- and V-MOF-74 can have an enhanced affinity compared to Mg-MOF-74 by 6–9 kJ/mol. Electronic structure calculations suggest that the origin of the major affinity trend is the local electric field effect of the open metal site that stabilizes CO_2, but forward donation from the lone-pair electrons of CO_2 to the empty d-levels of transition metals as in a weak coordination bond makes Ti and V have an even higher binding strength than Mg, Ca, and Sc.

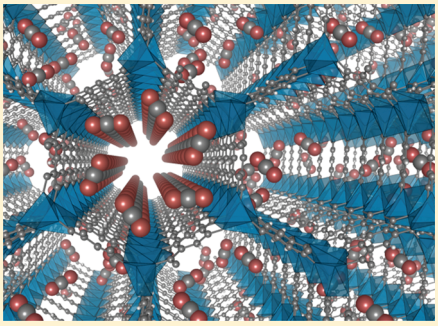

SECTION: Molecular Structure, Quantum Chemistry, General Theory

To lower the atmospheric CO_2 levels, there are attempts to prevent anthropogenic carbon emission prior to their release.[1−5] Although amine solutions such as monoethanolamine (MEA) are still widely used in industry, their recovery costs are very high, and they are notably corrosive. As an alternative, diverse porous adsorbents such as porous carbons,[6] zeolites,[7] boron nitride nanotube,[8] and metal–organic frameworks (MOFs)[9] are under consideration for the reversible capture and release of CO_2. In particular, due to the versatile structural properties (e.g., porosity and surface area) of MOFs that can be easily tuned by changing inorganic struts or organic linkers, MOFs have recently attracted a wide interest for gas sorption such as CO_2, H_2,[10−13] O_2,[10] and so forth. Indeed, MOF-210[14] and NU-100[15] with ultrahigh porosity of ∼6200 m^2/g shows an exceptional CO_2 capacity of >2800 mg/g at 298 K and 40 bar.

The combined experimental and modeling approaches recently showed that M-MOF-74 (M = Mg,[16] Ni,[17] Co,[18] Zn,[19] and Mn[20]) yields a much higher CO_2 uptake at 298 K and 0.1 bar than several other MOFs such as HKUST, ZIF-8, MOF-177, and so forth.[9] MOF-74 is constructed from the infinite helical secondary building units and 2,5-dioxido-1,4-benzenedicarboxylate (DOBDC) organic linkers to give a one-dimensional hexagonal tunnel with a micropore of ca. 1.3 nm in diameter, shown in Figure 1a. Each metal has a square pyramidal coordination with one coordinatively unsaturated (open) site toward an empty channel that can hold a gas molecule. Such an advantage of MOF-74 analogues for CO_2 capture results from a high CO_2 affinity. In particular, Mg-MOF-74 shows an experimental CO_2 affinity of 47 kJ/mol, which was attributed to a strong ionic character of Mg–O bonds.[16,21−23] Also, the MOF-74 types have a superior water stability compared to other MOFs.[24] For these reasons, the MOF-74 is presently considered as one of the more promising candidates for CO_2 capture.

For postcombustion CO_2 capture from flue gas, the required temperature and pressure conditions are 50–75 °C and 1 bar, respectively.[1] On the other hand, for precombustion capture, a high pressure of 30 bar is required at 40 °C.[1] Generally, the amount of CO_2 uptake in MOFs at high pressure (e.g., 30 bar) is correlated with the pore volume of MOFs,[14] indicating that MOFs with ultrahigh porosity such as MOF-210 and NU-100 would be desirable for the precombustion process. However, the CO_2 uptake at low pressure (e.g., 1 bar) is usually associated with the CO_2 binding affinity.[25] Thus, for the postcombustion process, MOFs with high CO_2 affinity, such as Mg-MOF-74, would be more desirable. Moreover, due to a need for high temperature, one needs MOFs with strong CO_2 affinity for efficient postcombustion capture.

On the basis of these considerations, therefore, it is clear that an increased affinity of CO_2 in the MOF-74 is the key to designing a more efficient CO_2 capture media. In this work, we tuned M-MOF-74 analogues for enhancing the CO_2 affinity by metal substitution, where we considered M = Mg, Ca, and the first transition metal elements (Sc, Ti, V, Cr, Mn, Fe, Co, Ni, Cu, and Zn). Our results suggest that Ti- and V-MOF-74 have higher CO_2 binding affinity than Mg-MOF-74, and that the origin of such a strong binding is a local electric field generated

Received: January 12, 2012
Accepted: March 4, 2012

   dx.doi.org/10.1021/jz300047n | J. Phys. Chem. Lett. 2012, 3, 826–829

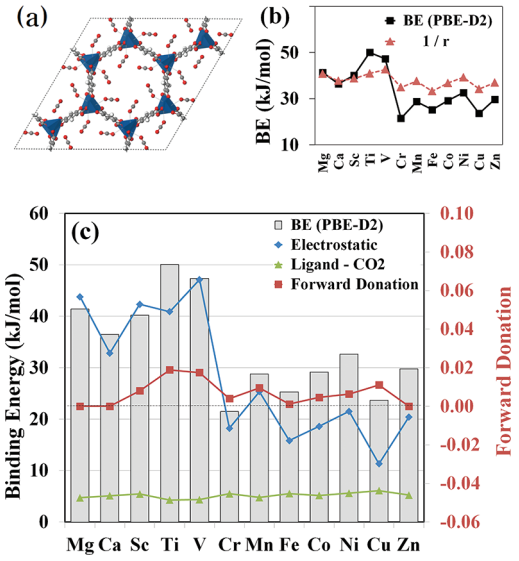

Figure 1. (a) Optimized hexagonal structure (PBE-D2) of Ti-MOF-74 binding with CO_2 (Ti, blue square pyramid; C, gray; O, red; H, white). (b) A correlation of the binding energy with the distance, r(M-OCO), between the metal and CO_2. (c) The CO_2 binding energies (gray bar), electrostatic energies scaled by 0.4 (blue line), CO_2−organic interaction energies (green line), and the charge transferred from the lone-pair of CO_2 to the empty d-levels of metal (red line against the y-axis on the right).

by a positive charge of the open metal site that stabilizes CO_2 and orbital interactions of the lone-pair of CO_2 with the empty d-levels of metals as in a coordination bond.

We calculated the binding energy of CO_2 with M-MOF-74 (M = Mg, Ca, and the first transition metal series) using density functional theory (DFT) with dispersion correction (D2)[27] in VASP.[28] The three-dimensional structures of M-MOF-74 were optimized in rhombohedral crystal structure using the Perdew−Burke−Ernzerhof[29] (PBE) exchange-correlation functional. We used the energy cutoff of 520 eV and 2 × 2 × 2 k-point sampling, and for DOS analysis 4 × 4 × 4 k-points were used. As seen in Table 1, the local density approximation (LDA) does not reproduce the experimental trend[16] of the binding affinity Mg > Ni > Co, while the generalized gradient approximation (GGA) such as Perdew−Wang 91[30] (PW91, Table S3) and the PBE exchange-correlation functional without dispersion correction significantly underestimates the overall binding by almost 50% compared to experiments. By contrast, the PBE with dispersion (PBE-D2) yields reasonable absolute binding energies (6−8 kJ/mol error compared to Caskey et al's experiments,[16] or 2 kJ/mol error compared to Britt et al's experiments[26]) and also reproduces the experimental trend for Mg, Ni, and Co correctly, hence used here for further discussions. Although a recent report[31] suggested that the use of DFT with empirical dispersion corrections might still lack sufficient accuracy to fully describe the interactions of water with the coordinatively unsaturated transition metal sites in MOFs, our case clearly indicates that the performance of DFT +D methods is system dependent and can indeed yield reliable results as compared to experiments (in particular if the focus is a relative binding affinity for similar compounds). We also note an experimental uncertainty (39 vs 47 kJ/mol) between the two sets[16,26] of experimental binding energies for Mg-MOF-74, suggesting that the experimental values for Co and Ni could also have related uncertainties. The cell parameters and atomic positions of empty M-MOF-74 analogues were fully relaxed. Six CO_2 molecules were then added in each primitive cel, and their atomic positions and cell sizes were reoptimized. As shown in Figure 1a, the CO_2 binding occurs via an end-on mode toward the open metal site. The bending of CO_2 molecules upon adsorption occurs to a minor extent with OCO angles of 178−180°. Lattice constants of optimized Mg-MOF-74 (a = 26.11, c = 6.91 Å) agree well with those of experiments (a = 26.02, c = 6.72 Å), although the volume of the unit cell varies for different metal substitution by −10% (Sc) to 15% (Ca) compared to an experimental Mg-MOF-74. Upon the binding of CO_2, we find no significant change in the magnetic moment of metals (Table S2).[32]

Table 1. The Calculated CO_2 Binding Energies (in kJ/mol) of M-MOF-74 and Distances (r, in Å) between the Metal and Oxygen of CO_2 (M−OCO) Using the PBE-D2 Method

	r(M−O)	LDA	PBE	PBE-D2	exp[16]
Mg	2.45	46.9	20.8	41.4	47 (39[26])
Ca	2.65	36.5	22.7	36.5	
Sc	2.58	46.8	16.3	40.2	
Ti	2.44	43.3	25.8	50.1	
V	2.34	57.6	25.4	47.3	
Cr	2.86	25.8	6.2	21.5	
Mn	2.66	33.6	12.2	28.8	
Fe	3.01	25.0	7.9	25.3	
Co	2.72	32.6	9.9	29.2	37
Ni	2.55	16.6	12.1	32.6	41
Cu	2.92	22.8	5.4	23.7	
Zn	2.71	34.0	11.8	29.8	

We find that Ti- and V-MOF-74s have higher binding affinities for CO_2 than Mg-MOF-74 by 6−9 kJ/mol, suggesting that they could be a more promising CO_2 capture medium than Mg-MOF-74. A strong correlation (Figure 1b) is observed between the binding energies and the distance ($1/r$) between the metal and the oxygen of CO_2 that points toward the metal, as in the binding of H_2 with MOF-74.[15]

To understand the origin of the different CO_2 binding affinity of MOF-74 with metal substitutions, we investigated the changes in electronic structure of various MOF-74 before and after the adsorption of CO_2. Figure 2 shows for Ti-MOF-74 (but generally true for all MOFs studied here, as shown in Figure S3), that the change in total density of states (TDOS) upon adsorption of CO_2 correlates very strongly with the shift of local density of states (LDOS) of CO_2 to lower energies (Figure 2a). The occupied electronic structure of a metal is, however, not altered to any noticeable degree after binding (Figure 2b), although the virtual levels do show some changes (Figure S6).

To assess the local electrostatic effects due to a positive charge developed on the open metal sites interacting with CO_2, we calculated the energy of CO_2 in the absence and presence of a point charge of the metal in its optimized distance using the RIMP2/cc-pVTZ method in Q-CHEM.[33] The partial charges of metals within the periodic MOF were obtained using the Bader analysis[34](Table S2). As shown in Figure 1c, the overall trend of the increased CO_2 stability in the presence of a simple external point charge (blue line) shows a very good agreement with the actual total interaction energies of CO_2 with various MOFs (bar graphs). In fact, all orbitals of CO_2 (including core and unoccupied levels) are stabilized inside the framework with

dx.doi.org/10.1021/jz300047n | J. Phys. Chem. Lett. 2012, 3, 826−829

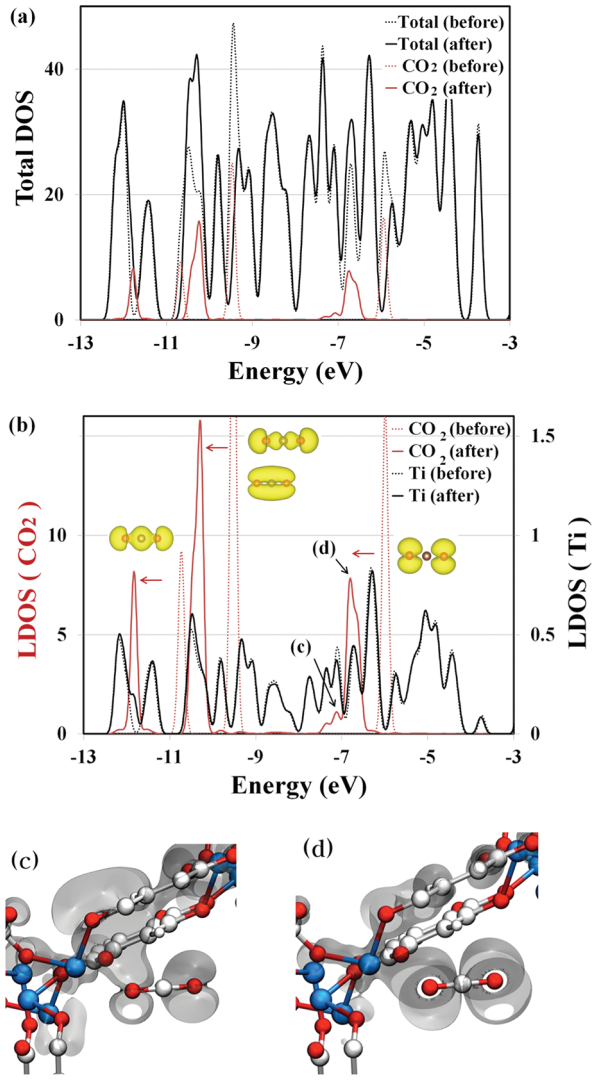

Figure 2. (a) TDOS before and after the CO_2 adsorption. The decreased and increased areas in TDOS after the adsorption overlap with those of the CO_2 peaks before and after the adsorption. (b) LDOS of CO_2 and metal (Ti) are shown. Three CO_2 peaks correspond to the highest occupied molecular orbital (HOMO), and the HOMO-1 and HOMO-2 molecular orbitals, respectively, where the HOMO corresponds to the nonbonding lone-pair of oxygen. The two DOSs before and after the adsorption of CO_2 are aligned by matching the core orbitals of hydrogen that is not involved in the binding. The DOSs shown are the summation of spin-up and spin-down components. In panels c and d, plotted are the charge densities at $E = -7.3$ and -6.7 eV, respectively, which show the orbital mixing of the lone-pair of CO_2 with the organic linker and the lone-pair with the metal site. Colors: blue for Ti, white for C and H (large and small balls, respectively), and red for O.

lower energies as compared to isolated CO_2, suggesting that the primary source of CO_2 binding with the MOF-74 is an external source such as the local electric field due to a positive charge of the open metal site.

This simple electric field effect cannot clearly explain the entire trend (in particular for Ti) since there are orbital interactions of CO_2 with the empty d-levels of metals as well as the π-structures of organic linkers, as shown in Figure 2c,d. Broadening and a further left-shift of the occupied CO_2 levels and the right-shift of some empty d-levels of metals are indicative of these orbital mixing (Figure S6).

To estimate the effects of organic linker for the CO_2 binding to MOF, we calculated the binding energy of CO_2 with the hydrogen-terminated organic linker at its optimized geometry (from Figure 1a) using RIMP2/cc-pVTZ with counterpoise correction for basis set superposition error (BSSE). The CO_2 is located on the oxido-group rather than the carboxylic-group of the linker (Figure S4). For all optimized M-MOF-74 structures, the organic$-CO_2$ interaction energies were similar and ~5 kJ/mol (green line in Figure 1c).

The mixing of lone-pair orbitals of CO_2 with the empty metal d-levels can be interpreted as a forward donation of electrons from a "ligand" to a metal as in a coordination bond. In fact, the latter orbital interaction responsible for the forward donation can also be clearly seen by a shift of the empty d-levels of the metal to a higher energy (Figure S6). In Figure 1c, the red line shows the amount of electrons added to the metal from the lone pair electrons of CO_2 due to this weak coordinative forward donation (Table S4 for technical details). Early transition metals such as Ti and V show the highest charging with 0.0189 and 0.0175 e^-, respectively, whereas Mg, Ca, and Sc show 0−0.0080 e^-. We note that forward donation can also decrease the partial positive charge of the metal, yielding a reduced electrostatic contribution to the binding energy. Thus, both local electric field effects and orbital interactions are needed to explain the affinity trend in Figure 1c satisfactorily.

In conclusion, we have shown that MOF-74 can be tuned to have a stronger binding affinity for CO_2 by metal substitution. Ti-MOF-74 and V-MOF-74 are predicted to be the more promising CO_2 scavengers. Uniform shift of the occupied levels of CO_2 in the DOS analysis shows that a simple electric field effect of the open metal site is the key that can explain the overall affinity trend across the third-row elements. Transition metals such as Ti and V form additional weak coordination bonds with CO_2 through forward donation, which then make the latter metals have an even higher binding energy than Mg. Since some of these transition metals often (but not always) prefer higher oxidation states than +2 as assumed here in the MOF-74 framework, demonstration of synthetic feasibility and assessment of theoretical predictions from the experimental sides have yet to be seen.

■ ASSOCIATED CONTENT

Supporting Information

Calculation details, calculated structural parameters, electrostatic energy estimations, DOS analyses for all metals before and after the binding of CO_2, charge densities for showing orbitals interactions, Bayder charge analysis, and forward donation analysis are described. This material is available free of charge via the Internet at http://pubs.acs.org.

■ AUTHOR INFORMATION

Corresponding Author

*Phone: +82-42-350-1712. FAX: +82-42-350-1710. E-mail address: ysjn@kaist.ac.kr.

Notes

The authors declare no competing financial interest.

■ ACKNOWLEDGMENTS

We are pleased to acknowledge the support of the Korea CCS R&D Center, Basic Science Research (2010-0023018), and WCU program (R31-2008-000-10055-0) funded by the Ministry of Education, Science and Technology of the Korean

government. We would like to thank Prof. Omar Yaghi for helpful discussions and kindness to share ongoing experiments on MOF-74 by his group related to our theoretical predictions. The generous supercomputing time from KISTI is gratefully acknowledged.

REFERENCES

(1) D'alessandro, D.; Smit, B.; Long, J. R. Carbon Dioxide Capture: Prospects for New Materials. *Angew. Chem., Int. Ed.* **2010**, *49*, 6058−6082.
(2) Yamasaki, A. An Overview of CO_2 Mitigation Options for Global Warming − Emphasizing CO_2 Sequestration Options. *J. Chem. Eng. Jpn.* **2003**, *36*, 361−375.
(3) Yang, H.; Xu, Z.; Fan, M.; Gupta, R.; Slimane, R.; Bland, A.; Wright, I. Progress in Carbon Dioxide Separation and Capture: A Review. *J. Environ. Sci.* **2008**, *20*, 14−27.
(4) Feron, P.; Hendriks, C. CO_2 Capture Process Principles and Costs. *Oil Gas Sci. Technol.* **2005**, *60*, 451−459.
(5) Keskin, S.; van Heest, T. M.; Sholl, D. S. Can Metal−Organic Framework Materials Play a Useful Role in Large-Scale Carbon Dioxide Separations? *ChemSusChem* **2010**, *3*, 879−891.
(6) Xu, X.; Song, C.; Andresen, J. M.; Miller, B. G.; Scaroni, A. W. Novel Polyethylenimine-Modified Mesoporous Molecular Sieve of MCM-41 Type as High-Capacity Adsorbent for CO_2 Capture. *Energy Fuels* **2002**, *16*, 1463−1469.
(7) Franchi, R. S.; Harlick, P. J. E.; Sayari, A. Applications of Pore-Expanded Mesoporous Silica. 2. Development of a High-Capacity, Water-Tolerant Adsorbent for CO_2. *Ind. Eng. Chem. Res.* **2005**, *44*, 8007−8013.
(8) Choi, H.; Park, Y. C.; Kim, Y.-H.; Lee, Y. S. Ambient Carbon Dioxide Capture by Boron-Rich Boron Nitride Nanotube. *J. Am. Chem. Soc.* **2011**, *133*, 2084−2087.
(9) Yazaydin, A. Ö.; Snurr, R. Q.; Park, T.-H.; Koh, K.; Liu, J.; Levan, M. D.; Benin, A. I.; Jakubczak, P.; Lanuza, M.; Galloway, D. B.; et al. Screening of Metal−Organic Frameworks for Carbon Dioxide Capture from Flue Gas Using a Combined Experimental and Modeling Approach. *J. Am. Chem. Soc.* **2009**, *131*, 18198−18199.
(10) Kim, Y.-H.; Sun, Y. Y.; Choi, W. I.; Kang, J.; Zhang, S. B. Enhanced Dihydrogen Adsorption in Symmetry-Lowered Metal-Porphyrin-Containing Frameworks. *Phys. Chem. Chem. Phys.* **2009**, *11*, 11400−11403.
(11) Sun, Y. Y.; Kim, Y.-H.; Zhang, S. B. Effect of Spin State on the Dihydrogen Binding Strength to Transition Metal Centers in Metal−Organic Frameworks. *J. Am. Chem. Soc.* **2007**, *129*, 12606−12607.
(12) Choi, W. I.; Jhi, S.-H.; Kim, K.; Kim, Y.-H. Divacancy-Nitrogen-Assisted Transition Metal Dispersion and Hydrogen Adsorption in Defective Graphene: A First-Principles Study. *Phys. Rev. B* **2010**, *81*, 085441.
(13) Kim, Y.-H.; Kang, J.; Wei, S.-H. Origin of Enhanced Dihydrogen−Metal Interaction in Carboxylate Bridged Cu_2−Paddle-Wheel Frameworks. *Phys. Rev. Lett.* **2010**, 105.
(14) Furukawa, H.; Ko, N.; Go, Y. B.; Aratani, N.; Choi, S. B.; Choi, E.; Yazaydin, A. O.; Snurr, R. Q.; O'Keeffe, M.; Kim, J.; et al. Ultrahigh Porosity in Metal−Organic Frameworks. *Science* **2010**, *329*, 424−428.
(15) Farha, O. K.; Yazaydın, A. Ö.; Eryazici, I.; Malliakas, C. D.; Hauser, B. G.; Kanatzidis, M. G.; Nguyen, S. T.; Snurr, R. Q.; Hupp, J. T. De Novo Synthesis of a Metal−Organic Framework Material Featuring Ultrahigh Surface Area and Gas Storage Capacities. *Nat. Chem.* **2010**, *2*, 944−948.
(16) Caskey, S. R.; Wong-Foy, A. G.; Matzger, A. J. Dramatic Tuning of Carbon Dioxide Uptake via Metal Substitution in a Coordination Polymer with Cylindrical Pores. *J. Am. Chem. Soc.* **2008**, *130*, 10870−10871.
(17) Dietzel, P. D. C.; Panella, B.; Hirscher, M.; Blom, R.; Fjellvåg, H. Hydrogen Adsorption in a Nickel Based Coordination Polymer with Open Metal Sites in the Cylindrical Cavities of the Desolvated Framework. *Chem. Commun.* **2006**, 959−961.
(18) Dietzel, P. D. C.; Morita, Y.; Blom, R.; Fjellvåg, H. An in Situ High-Temperature Single-Crystal Investigation of a Dehydrated Metal−Organic Framework Compound and Field-Induced Magnetization of One-Dimensional Metal−Oxygen Chains. *Angew. Chem., Int. Ed.* **2005**, *44*, 6354−6358.
(19) Rosi, N. L.; Kim, J.; Eddaoudi, M.; Chen, B.; O'Keeffe, M.; Yaghi, O. M. Rod Packings and Metal−Organic Frameworks Constructed from Rod-Shaped Secondary Building Units. *J. Am. Chem. Soc.* **2005**, *127*, 1504−1518.
(20) Zhou, W.; Wu, H.; Yildirim, T. Enhanced H_2 Adsorption in Isostructural Metal−Organic Frameworks with Open Metal Sites: Strong Dependence of the Binding Strength on Metal Ions. *J. Am. Chem. Soc.* **2008**, *130*, 15268−15269.
(21) Wilmer, C. E.; Snurr, R. Q. Towards Rapid Computational Screening of Metal−Organic Frameworks for Carbon Dioxide Capture: Calculation of Framework Charges via Charge Equilibration. *Chem. Eng. J.* **2010**, *171*, 775−781.
(22) Wu, H.; Simmons, J. M.; Srinivas, G.; Zhou, W.; Yildirim, T. Adsorption Sites and Binding Nature of CO_2 in Prototypical Metal−Organic Frameworks: A Combined Neutron Diffraction and First-Principles Study. *J. Phys. Chem. Lett.* **2010**, *1*, 1946−1951.
(23) Valenzano, L.; Civalleri, B.; Chavan, S.; Palomino, G. T.; Areán, C. O.; Bordiga, S. Computational and Experimental Studies on the Adsorption of CO, N_2, and CO_2 on Mg-MOF-74. *J. Phys. Chem. C* **2010**, *114*, 11185−11191.
(24) Han, S. S.; Choi, S.-H.; van Duin, A. C. T. Molecular Dynamics Simulations of Stability of Metal−Organic Frameworks against H_2O Using the ReaxFF Reactive Force Field. *Chem. Commun.* **2010**, *46*, 5713−5715.
(25) Babarao, R.; Jiang, J. Molecular Screening of Metal−Organic Frameworks for CO_2 Storage. *Langmuir* **2008**, *24*, 6270−6278.
(26) Britt, D.; Furukawa, H.; Wang, B.; Glover, T. G.; Yaghi, O. M. Highly Efficient Separation of Carbon Dioxide by a Metal−Organic Framework Replete with Open Metal Sites. *Proc. Natl. Acad. Sci. U.S.A.* **2009**, *106*, 20637−20640.
(27) Moellmann, J.; Grimme, S. Importance of London Dispersion Effects for the Packing of Molecular Crystals: A Case Study for Intramolecular Stacking in a Bis-Thiophene Derivative. *Phys. Chem. Chem. Phys.* **2010**, *12*, 8500−8504.
(28) Sun, G.; Kürti, J.; Rajczy, P.; Kertesz, M.; Hafner, J.; Kresse, G. Performance of the Vienna Ab Initio Simulation Package (VASP) in Chemical Applications. *J. Mol. Struct. (THEOCHEM)* **2003**, *624*, 37−45.
(29) Perdew, J. P.; Burke, K.; Ernzerhof, M. Generalized Gradient Approximation Made Simple. *Phys. Rev. Lett.* **1996**, *77*, 3865−3868.
(30) Perdew, J. P.; Chevary, J. A.; Vosko, S. H.; Jackson, K. A.; Pederson, M. R.; Singh, D. J.; Fiolhais, C. Atoms, Molecules, Solids, and Surfaces: Applications of the Generalized Gradient Approximation for Exchange and Correlation. *Phys. Rev. B* **1992**, *46*, 6671−6687.
(31) Grajciar, L.; Bludský, O.; Nachtigall, P. Water Adsorption on Coordinatively Unsaturated Sites in CuBTC MOF. *J. Phys. Chem. Lett.* **2010**, *1*, 3354−3359.
(32) Ohba, M.; Yoneda, K.; Agustí, G.; Muñoz, M. C.; Gaspar, A. B.; Real, J. A.; Yamasaki, M.; Ando, H.; Nakao, Y.; Sakaki, S.; et al. Bidirectional Chemo-switching of Spin State in a Microporous Framework. *Angew. Chem., Int. Ed.* **2009**, *48*, 4767−4771.
(33) Shao, Y.; Molnar, L. F.; Jung, Y.; Kussmann, J.; Ochsenfeld, C.; Brown, S. T.; Gilbert, A. T. B.; Slipchenko, L. V.; Levchenko, S. V.; O'Neill, D. P.; et al. Advances in Methods and Algorithms in a Modern Quantum Chemistry Program Package. *Phys. Chem. Chem. Phys.* **2006**, *8*, 3172−3191.
(34) Bader, R. F. W. *Atoms in Molecules - A Quantum Theory*; Oxford University Press: New York, 1990.